

Correlations and the Cross Section of Exclusive $(e, e'p)$ Reactions for ^{16}O

K. Amir-Azimi-Nili, J.M. Udias*, H. Mütter
*Institut für Theoretische Physik,
Universität Tübingen, D-72076 Tübingen, Germany*

L.D. Skouras
*Institute of Nuclear Physics, N.C.S.R. Demokritos
Aghia Paraskevi GR 15310, Greece*

A. Polls
*Departament d'Estructura i Constituents de la Matèria
Universitat de Barcelona, E-08028 Barcelona, Spain*

The reduced cross section for exclusive $(e, e'p)$ reactions has been studied in DWIA for the example of the nucleus ^{16}O using a spectral function containing effects of correlations. The spectral function is evaluated directly for the finite nucleus starting from a realistic nucleon-nucleon interaction within the framework of the Green's function approach. The emphasis is focused on the correlations induced by excitation modes at low energies described within a model-space of shell-model configurations including states up to the sdg shell. Cross sections for the p -wave quasi-hole transitions at low missing energies are presented and compared with the most recent experimental data. In the case of the so-called perpendicular kinematics the reduced cross section derived in DWIA shows an enhancement at high missing momenta as compared to the PWIA result. Furthermore the cross sections for the s - and d -wave quasi-hole transitions are presented and compared to available data at low missing momenta. Also in these cases, which cannot be described in a model without correlations, a good agreement with the experiment is obtained.

I. INTRODUCTION

The quasi-elastic $(e, e'p)$ reaction constitutes a very well suited tool to study the limitations of the simple shell-model or independent-particle model (IPM) of the nucleus. Indeed, it is now generally accepted that atomic nuclei are many-body systems in which correlations beyond the mean-field or Hartree-Fock picture play a significant role. It has been argued that the strong short-range and tensor components of realistic nucleon-nucleon (NN) interactions should induce short-range correlations into the nuclear wave function. These correlations should give rise to an enhancement in the momentum distribution of quasi-hole states at high momenta as compared to the momentum distribution derived from a Hartree-Fock or mean field description of the nucleus. Therefore high-resolution $(e, e'p)$ experiments have been performed to determine the spectral function of nucleons at high momenta leading to the ground-state or states with low excitation energies in the daughter nucleus [1,2].

Microscopic calculations, which account for the effects of these short-range correlations, indeed predict components in the momentum distribution at momenta around $2\text{-}3\text{ fm}^{-1}$, which are larger by orders of magnitude as compared to the predictions of Hartree-Fock or IPM calculations. These high-momentum components, however, mainly originate from the spectral function at large missing energies, leading to configurations of the $(A-1)$ particle system at energies above the threshold of particle emission for another nucleon. The momentum distribution for nucleons at low missing energies, which can be explored in exclusive $(e, e'p)$ reactions, seems not to be very sensitive to short-range correlations and may rather well be approximated by those derived from the IPM [3-8]. Similar results are also obtained in the study of the spectral function for nuclear matter [9-12].

This analysis was essentially confirmed by experiment. The experimental data for the reduced cross section in the light nucleus ^{16}O at low missing energies could be described reasonable well within the prediction of an IPM [1]. On the other hand, the momentum distribution for the heavy nucleus ^{208}Pb showed a small enhancement of high momentum components at low missing energies as compared to a Hartree-Fock or IPM prediction [2]. This enhancement is not as large as the one predicted from short-range correlations for the total momentum distribution including the contributions from high missing energies. It has been argued that this deviation from the IPM might be due to long-range correlations, which corresponds to low-energy excitations of the many-body system [2,13].

*Present address: Institute des Science Nuclaires, 53 Avenue des Martyrs, F-38026 Grenoble CEDEX (France)

The fact that this enhancement of the momentum distribution is observed for a heavy nucleus but not for the light nucleus ^{16}O supports the idea that the enhancement at small energies may originate from long-range correlations. The effects of short-range correlations should be rather independent of the nuclear system under consideration as these correlations are not very sensitive to the global structure of the whole nuclear system. Consequently the effects of short-range correlations should be rather similar for the nuclei ^{16}O and ^{208}Pb . Contrary long-range correlations could be sensitive to the whole nuclear system and exhibit different results for different nuclei. They are related to the excitation modes at low energy and therefore results derived from nuclear matter, which shows a continuous single-particle spectrum, can be quite different from those in finite nuclei, for which the low-energy excitations are rather sensitive to the shell-structure. Guided by these considerations we investigated long-range correlation effects in the spectral function and other related observables directly for the finite nucleus under consideration [14], as a study of nuclear matter may not be very reliable.

If one wants to study the effects of correlations by a comparison with experimental data, one has to employ the correlated wave function in a complete description of the $(e, e'p)$ reaction. Going beyond the Plane Wave Impuls Approximation the cross section cannot be factorized any longer into the elementary electron-proton cross section and the spectral function, exhibiting the effects of correlations. The reduced cross section calculated in the Distorted Wave Impuls Apoximation (DWIA) may contain effects of the final state interactions (FSI) and other effects which cannot be separated in this approach from the effects of correlations. Therefore a careful analysis has to be made of the different components entering in the computation of the reduced cross section.

Also we want to emphasize that one should investigate the reduced cross section leading to final states in the daughter nucleus, which are absent in the IPM. In the case of ^{16}O processes of this kind would be the knock-out of a nucleon leading to the $5/2$ and $1/2$ states of positive parity with low excitation energy in ^{15}N . In the IPM the $d_{5/2}$ and $1s_{1/2}$ states are not occupied and therefore the corresponding momentum distributions are not dominated by the quasi-hole part of the simple shell-model.

To account for long-range correlations a harmonic oscillator basis is used in order to determine the energies and the mixing of shell-model configurations. We consider that the low-energy excitation modes are adequately described within a model-space which includes all orbitals up to the sdg shell. A finite basis of oscillator states, however, is not at all appropriate to describe high-momentum components in the nuclear wave function, since these high-momentum components will be dominated by the tail of the oscillator basis states. Therefore, as we will explain below, we have used a mixed representation of basis states, which considers a shell-model basis to describe the excitation modes, but a basis of plane-wave states to determine the spectral function. The Green's function formalism for the nuclear many-body theory (for a reference see *e.g.* the recent review articles [15,16]) will be applied to evaluate the spectral function.

In Sec. II we will present the main points of the method we use to compute the correlated spectral function for ^{16}O . This part is followed in Sec. III by a brief summary of the formalism used to describe the $(e, e'p)$ reaction, where Coulomb distortion effects of the electron wave function and final state interaction of the outgoing proton are considered. The results for the reduced cross section for the different approximations and partial wave transitions are presented in Sec. IV. At the end we give a short review of our main conclusions.

II. THE SPECTRAL FUNCTION

The calculation of the cross section for exclusive $(e, e'p)$ reactions requires the knowledge of the hole spectral function. In the case of finite system it is convenient to introduce a partial wave decomposition which yields the spectral function for a nucleon in the single-particle basis with orbital angular momentum l , total angular momentum j , isospin τ and momentum k

$$S_{lj\tau}(k, k'; E) = \sum_n \langle \Psi_0^A | a_{k'lj}^\dagger | \Psi_n^{A-1} \rangle \langle \Psi_n^{A-1} | a_{klj\tau} | \Psi_0^A \rangle \delta(E - (E_0^A - E_n^{A-1})), \quad (1)$$

where $a_{klj\tau}$ ($a_{k'lj\tau}^\dagger$) denotes the corresponding annihilation (creation) operator. The state $|\Psi_0^A\rangle$ refers to the ground state of the target nucleus, while $|\Psi_n^{A-1}\rangle$ is used to identify the n th excited eigenstate of the hamiltonian with one particle removed from the target nucleus. Hence the hole spectral function in its diagonal form $S(\mathbf{k}, E)$ gives the probability of removing a particle with momentum \mathbf{k} from the target system of A particles leaving the resulting $(A-1)$ system with an energy $E^{A-1} = E_0 - E$, where E_0 is the ground state energy of the target. The spectral function for the various partial waves, $S_{lj\tau}(k, k', E)$ can be obtained from the imaginary part of the corresponding single-particle Green's function $g_{lj}(k_1, k_2, E)$. Note that here and in the following we have dropped the isospin quantum number τ , as we ignore the Coulomb interaction between the protons and study a symmetric nucleus with $N = Z$.

To determine the correlated single-particle Green's function one has to solve a Dyson equation, which using the partial wave representation appropriate for finite systems can be written as

$$g_{lj}(k_1, k_2; \omega) = g_{lj}^{(HF)}(k_1, k_2; \omega) + \int dk_3 \int dk_4 g_{lj}^{(HF)}(k_1, k_3; \omega) \Delta\Sigma_{lj}(k_3, k_4; \omega) g_{lj}(k_4, k_2; \omega), \quad (2)$$

where $g^{(HF)}$ refers to the Hartree-Fock propagator and $\Delta\Sigma_{lj}$ represents contributions to the irreducible self-energy, which go beyond the Hartree-Fock approximation for the nucleon self-energy used to derive $g^{(HF)}$. The hole spectral function S_{lj} can then be calculated easily from the imaginary part of the single-particle Green's function by

$$S_{lj}(k, k', \omega) = \frac{1}{\pi} \text{Imag}[g_{lj}(k, k'; \omega)]. \quad (3)$$

Although the evaluation of the Hartree-Fock approximation to the Green's function $g_{lj}^{(HF)}(k_1, k_2; \omega)$, the definition of $\Delta\Sigma_{lj}$ and the technique used to solve the Dyson Eq.(2) have been already discussed in detail in previous publication [17,14], we include a brief summary of the relevant aspects of this method.

A. Model space and effective hamiltonian

Long range correlations are taken into account by means of the Green's function approach within a finite model space. This model space shall be defined in terms of shell-model configurations including oscillator single-particle states up to the sdg shell. The oscillator parameter, $b = 1.76$ fm, has been chosen appropriate for the nucleus ^{16}O . This model space does not allow the description of short-range correlations. Nevertheless, we also have to take into account the effects of short-range correlations by introducing an effective interaction, *i.e.* a G -matrix appropriate for the model space. This truncation of the Hilbert space into a model space, the degrees of which are treated explicitly, and the space outside this model space, which is taken into account by means of effective operators, is often referred to as a double partitioned Hilbert space and has been used before for finite nuclei [18,19] and nuclear matter [20,21].

The G -matrix is determined as the solution of the Bethe-Goldstone equation

$$\mathcal{G} = V + V \frac{Q_{\text{mod}}}{\omega - Q_{\text{mod}} T Q_{\text{mod}}} \mathcal{G}, \quad (4)$$

where T is identified with the kinetic energy operator, while V stands for the bare two-body interaction. For the latter we have chosen the Reid soft-core potential [22]. In this equation the Pauli operator Q_{mod} is defined in terms of our harmonic oscillator single-particle states. Thus applying Q_{mod} to two-particle states $|\alpha\beta\rangle$ one obtains

$$Q_{\text{mod}}|\alpha\beta\rangle = \begin{cases} 0 & \text{if } \alpha \text{ or } \beta \text{ below Fermi level} \\ 0 & \text{if } \alpha \text{ and } \beta \text{ in model space} \\ |\alpha\beta\rangle & \text{elsewhere} \end{cases} \quad (5)$$

The model space used in the Eq. (4 and 5) includes all states up to the sdg-shell. Note that with this definition of Q_{mod} we ensure that no doublecounting of correlations occurs between the short-range correlations taken into account in the \mathcal{G} -matrix and the long-range correlations evaluated by means of the Green's function method within the model-space.

In the solution of the Bethe-Goldstone Eq.(4) we have chosen a constant value of $\omega = -30$ MeV for the starting energy. This value is a reasonable mean value for the sum of two single-particle energies for hole states in ^{16}O . Clearly, this choice is an approximation introduced to simplify the calculations, but one has to note that our results do not depend significantly on the actual value of ω . The use of a constant starting energy also implies that we do not try to account for a depletion of the occupation probability due to scattering into states outside the model space as it has been done *e.g.* in [23,24].

The matrix elements for \mathcal{G} are computed in a plane-wave basis for a specific finite nucleus and a corresponding model-space by expanding the techniques for solving the Bethe-Goldstone equation for finite systems as described in Ref. [25].

B. Nucleon Self-Energy and Green's Function

The calculation of the self-energy is performed in terms of two-particle states, characterized by single-particle momenta in the laboratory frame. Such a antisymmetrized 2-particle state would be described by quantum numbers such as

$$|k_1 l_1 j_1 k_2 l_2 j_2 J T \rangle \quad (6)$$

where k_i , l_i and j_i refer to momentum and angular momenta of particle i whereas J and T define the total angular momentum and isospin of the two-particle state. The transformation from the relative and c.m. coordinates, in which the matrix elements of \mathcal{G} are defined to the states displayed in Eq.(6) can be made by use of the well known vector bracket transformation coefficients [26,27].

Performing an integration over one of the k_i , one obtains a 2-particle state in a mixed representation of one particle in a bound harmonic-oscillator state while the other is in a plane-wave state

$$|n_1 l_1 j_1 k_2 l_2 j_2 J T \rangle = \int_0^\infty dk_1 k_1^2 R_{n_1 l_1}(b k_1) |k_1 l_1 j_1 k_2 l_2 j_2 J T \rangle. \quad (7)$$

Here $R_{n_1 l_1}$ stands for the radial oscillator function. An oscillator length $b = 1.76$ fm ($\hbar\omega = 13.3$ MeV) has been selected, which is an appropriate value to describe the bound single-particle states in ^{16}O . Now with the help of eqs.(6 - 7) we can write down our Hartree-Fock approximation for the self-energy in momentum representation

$$\Sigma_{l_1 j_1}^{HF}(k_1, k'_1) = \frac{1}{2(2j_1 + 1)} \sum_{n_2 l_2 j_2 J T} (2J + 1)(2T + 1) \langle k_1 l_1 j_1 n_2 l_2 j_2 J T | \mathcal{G} | k'_1 l_1 j_1 n_2 l_2 j_2 J T \rangle. \quad (8)$$

The summation over the oscillator quantum numbers is restricted to the states occupied in the IPM of ^{16}O . This Hartree-Fock part of the self-energy is real and does not depend on energy. One obtains the HF single-particle wave functions by expanding them

$$|\alpha^{HF} l j m \rangle = \sum_i |K_i l j m \rangle \langle K_i | \alpha^{HF} \rangle_{l j} \quad (9)$$

in a complete and orthonormal set of regular basis functions within a spherical box of radius R_{box} which is large compared to the radius of the nucleus

$$\Phi_{i l j m}(\mathbf{r}) = \langle \mathbf{r} | K_i l j m \rangle = N_{i l j} j_l(K_i r) \mathcal{Y}_{l j m}(\vartheta \varphi) \quad (10)$$

where $N_{i l}$ is an appropriate normalization constant, $\mathcal{Y}_{l j m}$ denotes the spherical harmonics including the spin degrees of freedom while j_l stands for the spherical Bessel functions with discrete momenta K_i determined from the boundary condition

$$j_l(K_i R_{\text{box}}) = 0. \quad (11)$$

The expansion coefficients of Eq.(9) are obtained by diagonalizing the HF Hamiltonian

$$\sum_{n=1}^N \langle K_i | \frac{K_i^2}{2m} \delta_{in} + \Sigma_{l j}^{HF} | K_n \rangle_{l j} \langle K_n | \alpha^{HF} \rangle_{l j} = \epsilon_{\alpha l j}^{HF} \langle K_i | \alpha^{HF} \rangle_{l j}. \quad (12)$$

Here and in the following the set of basis states in the box has been truncated by assuming an appropriate N . From the HF wave functions and energies one can construct the HF approximation to the single-particle Green's function in the box, which comes out as

$$g_{\alpha l j}^{(HF)}(k, k'; \omega) = \frac{\langle k | \alpha^{HF} \rangle_{l j} \langle \alpha^{HF} | k' \rangle_{l j}}{\omega - \epsilon_{\alpha l j}^{HF} \pm i\eta}. \quad (13)$$

Note that by choosing especially this basis we are able to separate contributions from different momenta to the HF single-particle state, which is essential in order to compute at the end of our formalism the single-particle Green's function in momentum space.

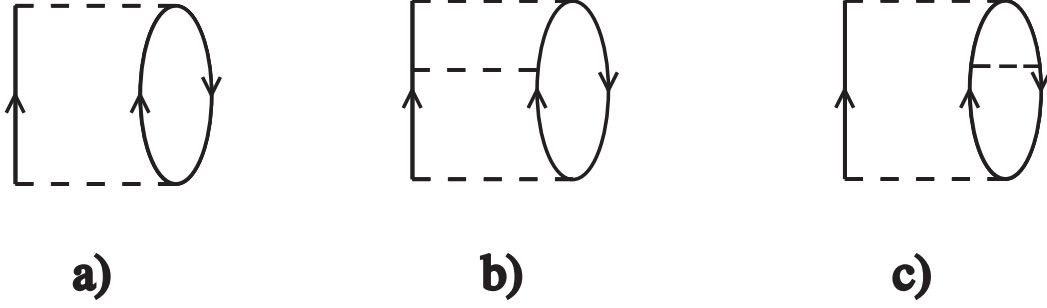


FIG. 1. Contributions to the nucleon self-energy of second (a) and third order in the interaction (b) and (c)

The next step in the evaluation of the irreducible self-energy is to take into account terms of second order in the effective interaction which correspond to intermediate 2-particle 1-hole (2p1h) states as displayed in Fig.1a)

$$\Sigma_{lj}^{(2p1h)}(k, k', \omega) = \frac{1}{2} \sum_{h < F} \sum_{p_1, p_2 > F} \frac{\langle kh | \mathcal{G} | p_1 p_2 \rangle \langle p_1 p_2 | \mathcal{G} | k' h \rangle}{\omega - e(p_1, p_2, h) + i\eta} \quad (14)$$

and intermediate 2-hole 1-particle (2h1p) states

$$\Sigma_{lj}^{(2h1p)}(k, k', \omega) = \frac{1}{2} \sum_{p > F} \sum_{h_1, h_2 < F} \frac{\langle kp | \mathcal{G} | h_1 h_2 \rangle \langle h_1 h_2 | \mathcal{G} | k' p \rangle}{\omega - e(h_1, h_2, p) - i\eta}. \quad (15)$$

Here we have introduced the abbreviation

$$e(\alpha, \beta, \gamma) = \epsilon_{\alpha}^{HF} + \epsilon_{\beta}^{HF} - \epsilon_{\gamma}^{HF} \quad (16)$$

where the $\epsilon_{\alpha, \beta, \gamma}^{HF}$ are the HF single-particle energies. Note that the summations in Eq.(14, 15) on particle labels like p_1, p_2 and p are restricted to those single-particle states within the model space, which are above the Fermi level (F), whereas the labels h_1, h_2 and h refer to hole states.

After the definition of the self-energy we can now proceed and calculate the corresponding single-particle Green's function g_{lj} by solving a Dyson equation (see Eq.(2)) with the g^{HF} taken from Eq.(13) and including the correlation effects contained in $\Delta\Sigma_{lj}$

$$\Delta\Sigma_{lj}(k, k', \omega) = \Sigma_{lj}^{(2p1h)}(k, k', \omega) + \Sigma_{lj}^{(2h1p)}(k, k', \omega). \quad (17)$$

C. Solution of the Dyson Equation

The technique we use to solve the Dyson equation in order to extract the basic ingredients of the single-particle Green's function is very similar to the one developed in [19,17,14]. So we will restrict ourselves in giving a short review of the basic steps towards the determination of the single-particle Green's function for a finite system within a model space of discrete single-particle states.

In order to obtain the information necessary for the Lehmann representation of the Green's function, we rewrite the Dyson equation as an eigenvalue problem [19]

$$\begin{pmatrix} H_{11}^0 & \dots & H_{1N}^0 & a_{11} & \dots & a_{1P} & A_{11} & \dots & A_{1Q} \\ \vdots & & \vdots & \vdots & & \vdots & \vdots & & \vdots \\ H_{N1}^0 & \dots & H_{NN}^0 & a_{N1} & \dots & a_{NP} & A_{N1} & \dots & A_{NQ} \\ a_{11} & \dots & a_{N1} & e_1 & & & 0 & & \\ \vdots & & \vdots & & \ddots & & & & \\ a_{1P} & \dots & a_{NP} & 0 & & e_P & & & 0 \\ A_{11} & \dots & A_{N1} & & & E_1 & & & \\ \vdots & & \vdots & & & & \ddots & & \\ A_{1Q} & \dots & A_{NQ} & 0 & \dots & 0 & \dots & E_Q & \end{pmatrix} \begin{pmatrix} X_{0,k_1}^n \\ \vdots \\ X_{0,k_N}^n \\ X_1^n \\ \vdots \\ X_P^n \\ Y_1^n \\ \vdots \\ Y_Q^n \end{pmatrix} = \omega_n \begin{pmatrix} X_{0,k_1}^n \\ \vdots \\ X_{0,k_N}^n \\ X_1^n \\ \vdots \\ X_P^n \\ Y_1^n \\ \vdots \\ Y_Q^n \end{pmatrix}, \quad (18)$$

where for simplicity we have dropped the corresponding conserved quantum numbers for parity and angular momentum (lj). The matrix to be diagonalized contains the HF hamiltonian defined in (12) and the coupling to the P different $2p1h$ configurations and Q $2h1p$ states which can be constructed in our model space with quantum numbers for parity and angular momentum j , which are compatible to the single-particle quantum numbers lj under consideration. As long as we are still ignoring any residual interaction between the various $2p1h$ and $2h1p$ configurations the corresponding parts of the matrix in (18) are diagonal with elements defined by e_i (E_j) for $2p1h$ ($2h1p$)

$$e_i = e(p_1, p_2, h) \quad E_j = e(h_1, h_2, p), \quad (19)$$

where we have used again the abbreviation (16). The matrix elements connecting the HF part to the additional states refer to

$$\begin{aligned} a_{mi} &= \langle k_m h | \mathcal{G} | p_1 p_2 \rangle \\ A_{mj} &= \langle k_m p | \mathcal{G} | h_1 h_2 \rangle \end{aligned} \quad (20)$$

Solving the eigenvalue problem (Eq.(18)) one gets as a result the single-particle Green's function in the Lehmann representation in the discrete basis of the box defined in Eq.(10). The eigenvalues ω_n define the position of the poles of the Green's function, which refer to the various states of the system with $A \pm 1$ nucleons and the corresponding spectroscopic amplitudes are given by

$$\begin{aligned} \langle \Psi_0^A | a_{k_i} | \Psi_n^{A+1} \rangle &= X_{0,k_i}^n \quad \text{for } \omega_n > E_F \\ \langle \Psi_0^A | a_{k_i}^\dagger | \Psi_n^{A-1} \rangle &= X_{0,k_i}^n \quad \text{for } \omega_n < E_F \end{aligned} \quad (21)$$

which depend on whether ω_n is an energy above or below the Fermi energy E_F . Note that the coefficients X_{0,k_i}^n in the above equations stand for the momentum representation of the quasi-hole (quasi-particle) wave functions. That means one can set $X_{0,k_i}^n = \Phi_{nlj}(k_i)$. With the help of this nomenclature we can finally write down the spectral function in momentum space for a given energy ω_n and a given partial wave

$$S_{lj}(k, k', \omega_n) = X_{0,k'}^{n*} X_{0,k}^n = \phi_{nlj}^*(k') \phi_{nlj}(k) \quad (22)$$

in a separable representation (compare Eq.(1)), which is important in order to be able to use the so computed spectral function in the description of ($e, e'p$) reactions. The corresponding spectroscopic factor $S_n(\omega_n)$ (compare Eq.(29)) for the removal of a particle of a given shell $\{nlj\}$ is determined by the norm of the quasi-hole wave function which reads according to the chosen box basis as

$$S_n(\omega_n) = \int_0^{R_{\text{box}}} dr r^2 |\Phi_{nlj}(r)|^2 = \sum_i |X_{0,k_i}^n|^2, \quad (23)$$

where $\Phi_{nlj}(r)$ stands for the Fourier-Bessel transform of $\phi_{nlj}(k)$.

In a straightforward way one can improve the approximation discussed so far and incorporate the effects of residual interactions between the $2p1h$ configurations as illustrated in the diagrams displaying the self energy in Fig. 1b) and c). The same holds for the $2h1p$ configurations. One simply has to modify the corresponding parts of the matrix in Eq.(18) and replace

$$\begin{pmatrix} e_1 & \dots & 0 \\ \vdots & \ddots & \\ 0 & \dots & e_P \end{pmatrix} \Rightarrow \mathcal{H}_{2p1h}, \quad \text{and} \quad \begin{pmatrix} E_1 & \dots & 0 \\ \vdots & \ddots & \\ 0 & \dots & E_Q \end{pmatrix} \Rightarrow \mathcal{H}_{2h1p}, \quad (24)$$

where \mathcal{H}_{2p1h} and \mathcal{H}_{2h1p} contain the residual interactions in the $2p1h$ and $2h1p$ subspaces. The solution of the eigenvalue problem also leads to a normalization condition, which ensures that

$$\sum_n |X_{0,k_i}^n|^2 + \sum_m |X_{0,k_i}^m|^2 = \sum_n |\langle \Psi_n^{A+1} | a_{k_i}^\dagger | \Psi_0^A \rangle|^2 + \sum_m |\langle \Psi_m^{A-1} | a_{k_i} | \Psi_0^A \rangle|^2 = 1, \quad (25)$$

where the sum on n accounts for all solutions with ω_n larger than the Fermi energy and the sum on m for all solutions with ω_n below the Fermi energy. Again this implies that one ignores all effects of correlations, which are due to configurations outside the model space, like *e.g.* an effective energy-dependent hamiltonian [23,24]. In that case one has to renormalize the condition of Eq.(25) as well.

Note that for the solution of the eigenvalue problem one can apply the so-called ‘‘Basis Generated by Lanczos’’ (BAGEL) scheme [19,17,28] in order to get a very efficient representation of the single-particle Green's function in terms of a few ‘‘characteristic’’ poles in the Lehmann representation.

III. REDUCED CROSS-SECTIONS

Reduced cross-sections for $(e, e'p)$ reactions on ^{16}O have recently been measured at NIKHEFK [29] in the region of missing momenta up to around 300 MeV and at MAMI in Mainz [1] including missing momenta up to 700 MeV. The simplest approximation to analyze the $(e, e'p)$ process is the Plane Wave Impulse Approximation (PWIA), where one makes the assumption that the proton is ejected from the nucleus without any further interaction with the residual nucleus. In nonrelativistic PWIA the differential cross section factorizes into two terms, the elementary electron-proton cross section, accounting for the interaction between the incident electron and the bound proton, and the spectral function that accounts for the probability to find a proton with given energy and momentum in the nucleus. Although the factorization is destroyed when one takes into account the distortion of the electron and/or outgoing proton waves, or a relativistic approach for the bound state, it is useful and common practice to analyze the results in terms of a reduced cross section defined in such a way that it would coincide with the spectral function if factorization were fulfilled. For selected values of the missing energy E_m (*i.e.* for selected quasi-hole excitations) the reduced cross section is given by

$$\rho(\mathbf{p}_m) = \int_{\Delta E_m} dE_m [\sigma^{ep}|\mathbf{p}_p|E_p]^{-1} \frac{d^6\sigma}{dE_p d\epsilon'_e d\Omega_p d\Omega'_e}, \quad (26)$$

with \mathbf{p}_m the experimental missing momentum ($= -P_{A-1}$), $E_p, |\mathbf{p}_p|, \Omega_p$ (ϵ'_e, Ω'_e) the outgoing proton (electron) kinematical variables, and experimentally, the integral is performed over the interval ΔE_m that contains the peak of the transition under study. The term σ^{ep} represents the elementary electron-proton cross section. The data of $\rho(\mathbf{p}_m)$ are obtained dividing the experimental cross section by σ_{cc1}^{ep} , as given by Eq.(17) of Ref. [30]. We therefore use the same expression for σ^{ep} in our theoretical calculations. In PWIA, $\rho(\mathbf{p}_m)$ represents the momentum distribution of the selected quasi-hole state α .

In this section we briefly summarize the formalism used to describe the $(e, e'p)$ reaction. More details can be found in Refs. [31–33]. We base our calculations on the impulse approximation (virtual photon absorbed by the detected nucleon), which is known [34] to be a reliable approximation at quasi-elastic kinematics. The basic equations that determine the reduced cross section are given explicitly in Refs. [31,32], in terms of the electron and nuclear currents. The calculations have been performed with the code developed by one of us [35].

We work in the laboratory frame in which the target nucleus is at rest and use the notation and conventions of Ref. [36]. We denote by $k_e^\mu = (\epsilon_e, \mathbf{k}_e)$ the four-momentum of the incoming electron and by $k'_e{}^\mu = (\epsilon'_e, \mathbf{k}'_e)$ the four-momentum of the outgoing one. The four-momentum of the exchanged photon is $q^\mu = k_e^\mu - k'_e{}^\mu = (\omega, \mathbf{q})$. $P_A^\mu = (M_A, \mathbf{0})$ and $P_{A-1}^\mu = (E_{A-1}, \mathbf{P}_{A-1})$ denote the four-momenta of the target and residual nucleus, while $p_p^\mu = (E_p, \mathbf{p}_p)$ is the four-momentum of the ejected proton.

Using plane waves for the electrons and considering knock-out from a given $\{nlj\}$ quasi-hole state, we write the amplitude for the $(e, e'p)$ process in DWIA as [32–34]:

$$W_{if} = \frac{m_e}{\sqrt{\epsilon_e \epsilon'_e}} \bar{u}(\mathbf{k}'_e, \sigma'_e) \gamma_\mu u(\mathbf{k}_e, \sigma_e) \frac{(-1)}{q_\mu^2} J_N^\mu(\omega, \mathbf{q}), \quad (27)$$

where $u(\mathbf{k}, \sigma)$ represent four-component relativistic free electron spinors [36], and $J_N^\mu(\omega, \mathbf{q})$ is the nuclear current

$$J_N^\mu(\omega, \mathbf{q}) = \overline{\sum}_I \sum_F \delta(E_F - E_I - \omega) \int d\mathbf{r} e^{i\mathbf{q}\cdot\mathbf{r}} \langle \Psi_A^F | \hat{J}_N^\mu | \Psi_A^I \rangle, \quad (28)$$

where the matrix element of the nuclear charge-current density operator is taken between the initial $|\Psi_A^I\rangle$ and the final $|\Psi_A^F\rangle$ nuclear states. The initial state will be given by the many-particle wave function of A bound particles in the ground state for the target nucleus $|\Psi_0^A\rangle$. For the final state, the experimental conditions dictate a state that behaves asymptotically as a knocked out nucleon with momentum p_p and a residual nucleus in a well-defined state $|\Psi_n^{A-1}(E)\rangle$ with energy E and quantum numbers n . It is possible [8,37] to describe the matrix element in Eq. (28) in terms of the simple one-body current operator sandwiched between the hole spectral functions

$$[S_n]^{1/2} \phi_{E_n}(\mathbf{p}) = \langle \Psi_n^{A-1}(E) | a(\mathbf{p}) | \Psi_0^A \rangle \quad (29)$$

and

$$\chi_{p_p E_n}^{(-)} = \langle \Psi_n^{A-1}(E) | a(\mathbf{p}) | \Psi_A^F \rangle \quad (30)$$

describing the overlap between the residual state $|\Psi_n^{A-1}(E)\rangle$ and the hole produced in $|\Psi_0^A\rangle$, and $|\Psi_A^F\rangle$ respectively, by removing a particle with momentum \mathbf{p} . The way to compute these overlaps was described in the previous section. Hence, we take ϕ_{E_n} normalized to 1, and $S_n(E)$ is the spectroscopic factor associated with the removal process.

One may perform a similar calculation for $\chi_{p_p E_n}^{(-)}$, the final (continuum) wave function of the ejected proton. Usually, however, this particle wave function is derived from a phenomenological local optical potential. Also in this work we compute the the wave function for the outgoing proton $\chi_{p_p E_n}^{(-)}$ as a scattering solution obtained from an optical potential in a relativistic framework fitted to elastic proton scattering data on ^{16}O [38]. No Perey factors are included, as the dependence on the energy of these potentials is very soft at the energies of interest.

To avoid expansions in p/M and the reductions of the current operator typical of the nonrelativistic approaches, the fully relativistic kinematics and structure of the operator is used. In order to do that, we build a 4-component spinor out of the nonrelativistic bispinor ϕ_{E_n} . Also, we use relativistic optical potentials [38], which according to previous results [32,39], seem to be more adequate for $(e, e'p)$ calculations. However, our calculation is essentially nonrelativistic and, in consistency with the derivation of the spectral functions, no contributions from the negative energy sector are allowed in neither the bound or scattered proton wave function. The results would be equivalent to the ones obtained with the nonrelativistic formalism and equivalent optical potentials, only that all orders of p/M are included in our calculation. We obtain similar results with a nonrelativistic prescription for the scattered states (nonrelativistic optical potentials and Perey factors), only the reduced cross-sections are slightly increased.

For the nucleon current operator we take the free nucleon expression

$$\hat{J}_N^\mu = F_1 \gamma^\mu + i \frac{\bar{\kappa} F_2}{2M} \sigma^{\mu\nu} q_\nu, \quad (31)$$

where F_1 and F_2 are the nucleon form factors related in the usual way [36] to the electric and magnetic Sachs form factors of the dipole form. As discussed in Refs. [32,40], DWIA results depend on the choice of the nucleon current operator. Here we have chosen the operator that is closer to the one used in the nonrelativistic calculations of the DWEEPY code, and most often employed.

The Coulomb distortion of the electron wave function is considered with an effective momentum approach. The value of the shift in the energy of the electron is obtained by comparing with the exact calculation (DWBA) [33] and it is set in this case to about 4 MeV. For a light nuclei as ^{16}O , this procedure is already sufficient in order to include this effect accurately in the cross-sections [41].

IV. RESULTS AND DISCUSSION

In the first part of this discussion we would like to emphasize the effects of the final state interaction for the outgoing proton. For this purpose Fig. 2 displays the reduced cross section, calculated in perpendicular kinematics for the $^{16}\text{O}(e, e'p)^{15}\text{N}$ reaction leading to the ground state $(1/2^-)$ of ^{15}N , as a function of missing momentum. Results are shown for three different momentum transfers q of the virtual photon. As a reference all three parts of this figure include the results of the PWIA. The PWIA yields a reduced cross section which is identical to the spectral function and independent on the momentum of the absorbed photon. Two different models have been employed to describe the distortion of the wave function of the outgoing proton. The first model is based on a microscopic Dirac-Brueckner-Hartree-Fock calculation for the nucleus ^{16}O [42]. This DWIA-RH (Relativistic Hartree) approach only yields a real part for the nucleon nucleus potential. The second approach (DWIA-ROP) also accounts for the absorption of the outgoing proton by means of inelastic scattering. Also the DWIA-ROP approach assumes a relativistic form of the optical potential. The scalar and vector terms for the real and imaginary part are obtained in a phenomenological way by a global fit of elastic proton-nucleus scattering data [38].

With the inclusion of the final state interaction, the cross section cannot be factorized any more into the free electron-nucleon cross section times a spectral function. Therefore the reduced cross sections displayed in Fig. 2 depend on the momentum q of the absorbed photon. The difference between the two-models of the final state interaction can mainly be attributed to the effects of the imaginary component in DWIA-ROP. The absorptive effects contained in this imaginary part leads to a reduction of the cross section (as compared to the DWIA-RH results) which seems to be rather insensitive with respect to the missing momentum p_m . Therefore in the following we will restrict the presentation of calculated cross sections to the DWIA-ROP approach.

The real part of the optical potential tends to smoothen the reduced cross section by shifting strength from small momenta to high missing momenta. Independent on the detailed form of the optical potential one also observes an increase of the reduced cross section with increasing photon momentum q .

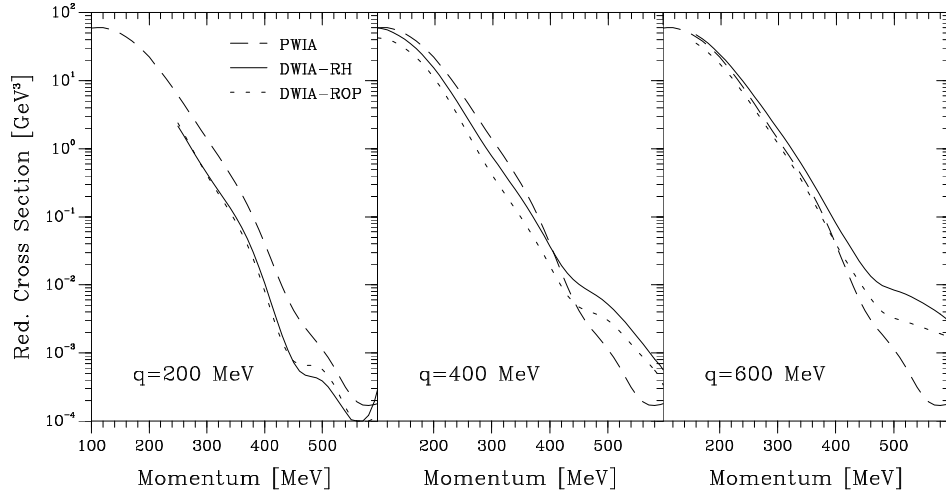


FIG. 2. Reduced cross section for the $^{16}\text{O}(e, e'p)^{15}\text{N}$ reaction leading to the ground state of ^{15}N in perpendicular kinematics. The results for PWIA are compared with those from DWIA calculated with a relativistic Hartree potential (RH) and a relativistic optical potential (ROP).

After exploring these features of the final state interaction, we now want to compare our results for the reduced cross sections with experimental data. In particular we would like to study how the effects of long-range correlations may affect the shape of the spectral function. The long-range correlations are described in terms of the 2p1h and 2h1p configurations within a model space including single-particle states up to the sdg shell and taking into account effects of the residual interaction between these configurations. For a more detailed discussion on the importance of contributions to the self-energy represented by diagrams of third and higher order in the residual interaction as displayed by Figs. 1b and 1c and their effects on the momentum distribution and other observables we refer to Ref. [14].

To observe the influence of long-range correlations on the momentum distribution, we present in Fig. 3 the reduced cross section for the $^{16}\text{O}(e, e'p)^{15}\text{N}$ reaction leading to the ground state ($1/2^-$) and first excited state ($3/2^-$) of ^{15}N . These have been calculated both with the fully correlated spectral function (Full) and also with our mean-field (HF) description (see Eq.(13)). The results are compared with the experimental data taken from the experiment at MAMI (Mainz) [1]. The underlying formalism to compute the reduced cross section is performed as described previously, where the phenomenological relativistic optical potential [38] was used. The relevant piece of the nuclear structure calculation for the proton knock-out reaction is the quasi-hole part of the fully correlated spectral function for the $p_{1/2}$ and $p_{3/2}$ partial wave presented in the previous chapter (see Eq.(22) and Eq.(24)). As we are mainly interested in the comparison of the data at high missing momenta with the predictions at low momenta, the corresponding spectroscopic factors $S_n(E)$ 0.60 ($0p_{1/2}$) and 0.45 ($0p_{3/2}$) were determined by a fit of the calculated cross section to the experimental results at small missing momenta deduced from the NIKHEF data [29]. These adjusted spectroscopic factors are significantly smaller than the theoretical values of 0.83 and 0.85 for the $p_{1/2}$ and $p_{3/2}$ states, respectively. For this comparison, however, one must keep in mind that these calculated spectroscopic factors only account for the effects of long-range correlations. Short-range correlations should lead to additional reduction by another factor of 0.8 and subnucleonic degrees of freedom may be responsible for the remaining discrepancy.

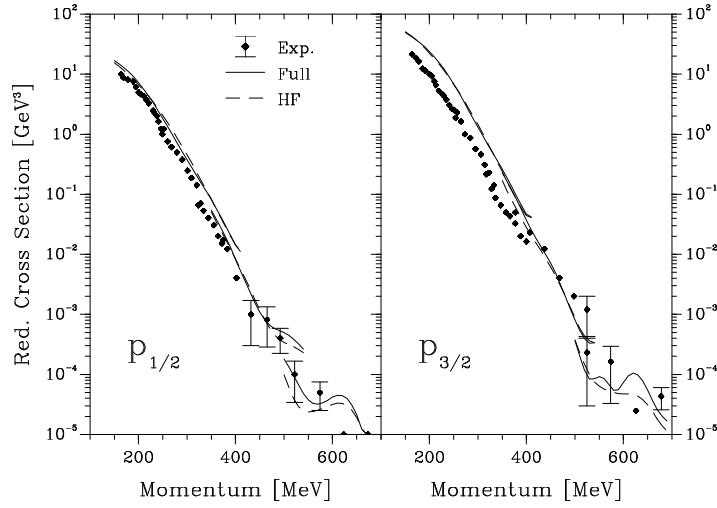


FIG. 3. Reduced cross section for the $^{16}\text{O}(e, e'p)^{15}\text{N}$ reaction leading to the ground state ($1/2^-$) and first excited state ($3/2^-$) of ^{15}N in the kinematical conditions considered in the experiment at MAMI (Mainz) [1]. Results for the mean-field description (HF) and the fully correlated spectral function (Full) are presented. The spectroscopic factors determined by a fit to low-p data from the NIKHEF experiment [29] are $S_{0p_{1/2}}=0.60$ (0.83) and $S_{0p_{3/2}}=0.45$ (0.85), where the values obtained by the theoretical approach are enclosed in parenthesis.

As one can clearly see in Fig. 3, the inclusion of long-range correlations does not lead to a significant enhancement of the reduced cross section at high missing momenta as compared to the predictions of the mean field or Hartree-Fock approach. This conclusion is not altered even in a complete description of the $(e, e'p)$ experiment including FSI and other effects. This statement confirms the result already obtained by an investigation of long-range correlations (*i.e.* correlations induced by excitation modes at low energies), on the energy and momentum distribution for the nucleus ^{16}O [14]. It should be emphasized, however, that a rather reasonable description of the reduced cross section is obtained over a large range of missing momenta with the adjustment of only one parameter, the spectroscopic factor, which has been adjusted to describe the NIKHEF data at small missing momenta.

Now one could argue that in the $(3/2^-)$ and $(1/2^-)$ case the spectral function has a dominant quasi-hole part originating from the corresponding hole (*i.e.* bound) state. Therefore any effects of correlations would be overwhelmed by this dominating quasi-hole component, which is present already in the Hartree-Fock approximation. This argument is supported by observing that in Fig. 3 the reduced cross section computed with the fully correlated spectral function does not differ substantially from the mean field description. In this sense it would be more interesting to investigate transitions to final states which do not have such a dominant quasi-hole part and would be impossible to describe within the mean field approximation. Best examples at low missing energies in ^{16}O is the case of the $d_{5/2}$ and $s_{1/2}$ hole states. As we are able to compute the fully correlated spectral functions also for these partial waves it would be worth comparing these results with corresponding experimental data. Unfortunately, until now we are not aware of data from the MAMI (Mainz) experiment [1] for high missing momenta of these partial waves. So we had to take the experimental data from the NIKHEF experiment in parallel kinematics [29] which cover only the momentum region up to 280 MeV/c. Moreover, they could not resolve the contributions from the $(5/2^+)$ and $(1/2^+)$ states. In Fig. 4 we display the results obtained for the reduced cross section taking the fully correlated spectral functions and assuming an incoherent sum of the $1/2^+$ and $5/2^+$ contributions for the $^{16}\text{O}(e, e'p)^{15}\text{N}$ reaction leading to the first excited state with positive parity ($1/2^+ - 5/2^+$ -doublet) of ^{15}N . The experimental data points are taken from the NIKHEF experiment [29] mentioned above.

Contrary to the previous case, the curves in Fig. 4 are scaled with the spectroscopic factors given by the theoretical approach, 0.055 ($s_{1/2}$) and 0.035 ($d_{5/2}$) respectively. The reasonable agreement with experiment shown in Fig. 4, means that the underlying microscopic calculation of the spectral function could be used to explore the high momentum region. Note that one could get better agreement with the experimental results by using the spectroscopic factors of 0.0357 ($s_{1/2}$) and 0.1140 ($d_{5/2}$) which have been obtained by fitting the experimental data [29]. In view of our aim to test our theoretical approach this has not been done here.

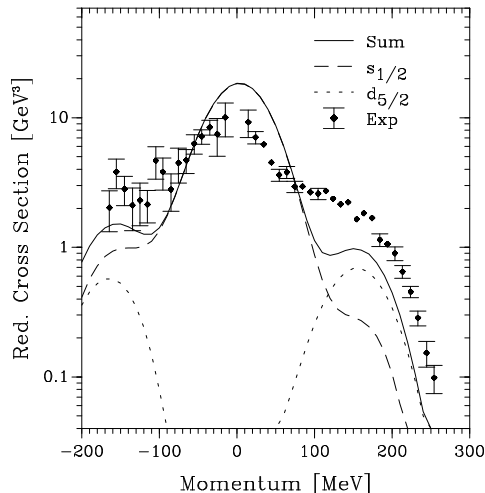


FIG. 4. Reduced cross section for the $^{16}\text{O}(e, e'p)^{15}\text{N}$ reaction leading to the first excited state with positive parity ($1/2^+ - 5/2^+$ -doublet) of ^{15}N in parallel kinematics. The experimental data are taken from NIKHEF experiment [29]. The corresponding spectroscopic factors $S_{s_{1/2}}=0.055$ and $S_{d_{5/2}}=0.035$ are taken from the theoretical approach.

V. CONCLUSIONS

The reduced cross section for the $(e, e'p)$ process has been studied in DWIA for the example of the nucleus ^{16}O using a spectral function containing long-range correlations. The fully correlated spectral function in the various partial waves is derived from the single-particle Green's function, which is obtained from the solution of a Dyson equation in basis of plane-wave states. The self-energy for the nucleons entering this Dyson equation contains the Brueckner-Hartree-Fock term plus the coupling to 2p1h and 2h1p configurations inside a model space with single-particle states up to the sdg shell. The long-range correlations are described in terms of these 2p1h and 2h1p configurations including the residual interaction among them.

Effects of final state interactions for the outgoing protons are included by means of relativistic optical model interactions. The effects of the final state interaction are non-negligible and spoil the factorization of the total cross section into the spectral function times the free electron-nucleon cross section. The effects of the final state interaction turn out to be rather insensitive to the specific choice of the optical model.

Including these effects of the final state interaction the calculated cross section for $(e, e'p)$ reactions leading to the $0p_{1/2}$ and $0p_{3/2}$ quasi-hole states in ^{16}O agree rather well with the experimental data [1] over a large range of missing momenta. It turns out, however, that these data are rather insensitive to correlation effects. Spectral functions derived from the Hartree-Fock approach yield an agreement of similar quality.

In order to investigate the effects of correlations, one should study $(e, e'p)$ reactions to final states, which are impossible within the mean field or Hartree-Fock approach. Examples for such states at low missing energies are the $5/2^+$ and $1/2^+$ states in ^{15}N . The cross section derived from the correlated single-particle Greens function is in good agreement with the experimental data.

VI. ACKNOWLEDGEMENTS

This project has been supported from the EC-program 'Human Capital and Mobility' under Contract N. CHRX-CT 93-0323. It has also received support by the "Sonderforschungsbereich SFB 382".

[1] K.I. Blomqvist et al., *Phys. Lett.* **344 B** (1995) 85.

[2] I. Bobeldijk et al., *Phys. Rev. Lett.* **73** (1994) 2684.

- [3] S.C. Pieper, R.B. Wiringa, and V.R. Pandharipande, *Phys. Rev.* **C46** (1992) 1741.
- [4] G. Co', A. Fabrocini, and S. Fantoni, *Nucl. Phys.* **A 568** (1994) 73.
- [5] O. Benhar, A. Fabrocini, S. Fantoni, and I. Sick, *Nucl. Phys.* **A579** (1994) 493.
- [6] H. Müther, A. Polls, and W.H. Dickhoff, *Phys. Rev.* **C 51** (1995) 3040.
- [7] H. Müther, and W.H. Dickhoff, *Phys. Rev.* **C 49** (1994) R17.
- [8] A. Polls, M. Radici, S. Boffi, W.H. Dickhoff and H. Müther, *Phys. Rev.* **C 55** (1997)
- [9] A. Ramos, A. Polls, and W.H. Dickhoff, *Nucl Phys.* **A503** (1989) 1.
- [10] O. Benhar, A. Fabrocini, and S. Fantoni, *Nucl. Phys.* **A505** (1989) 267.
- [11] B.E. Vonderfecht, W.H. Dickhoff, A. Polls, and A. Ramos, *Nucl. Phys.* **A 555** (1993) 1.
- [12] H. Müther, G. Knehr, and A. Polls, *Phys. Rev.* **C 52** (1995) 2955.
- [13] Z.Y. Ma and J. Wambach, *Phys. Lett.* **B 256** (1991) 1.
- [14] K. Amir-Azimi-Nili, H. Müther, L.D. Skouras, and A. Polls, *Nucl. Phys.* **A 604** (1996) 245.
- [15] C. Mahaux and R. Sartor, *Adv. Nucl. Phys.* **20** (1991) 1.
- [16] W.H. Dickhoff and H. Müther, *Rep. Prog. Phys.* **55** (1992) 1947.
- [17] H. Müther and L.D. Skouras, *Nucl. Phys.* **A 581** (1995) 247.
- [18] B.R. Barrett and M.W. Kirson, *Adv. in Nucl. Phys.* **6** (1973) 219
- [19] H. Müther and L.D. Skouras, *Nucl. Phys.* **A 555** (1993) 541.
- [20] T.T.S. Kuo, Z.Y. Ma and R. Vinh Mau, *Phys. Rev.* **C 33** (1987) 717.
- [21] M.F. Jing, T.T.S. Kuo and H. Müther, *Phys. Rev.* **C 38** (1988) 2408.
- [22] R.V. Reid, *Ann. of Phys.* **50** (1968) 411.
- [23] S.D. Yang and T.T.S. Kuo, *Nucl. Phys.* **A 456** (1986) 413.
- [24] K. Allaart, P.J. Ellis, W.J.W. Geurts, J. Hao, T.T.S. Kuo and G.A. Rijsdijk, *Phys. Rev.* **C74** (1993) 895.
- [25] H. Müther and P.U. Sauer, in *Computational Nuclear Physics 2* eds. K. Langanke, J.A. Maruhn and S.E. Koonin, page 30ff (Springer Verlag N.Y. 1993).
- [26] C.W. Wong and D. M. Clement, *Nucl. Phys.* **A 183** (1972) 210.
- [27] D. Bonatsos and H. Müther, *Nucl. Phys.* **A 496** (1989) 23.
- [28] H. Müther, T. Taigel and T.T.S. Kuo, *Nucl. Phys.* **A 482** (1988) 601.
- [29] M. Leuschner *et al.*, *Phys. Rev.* **C 49** (1994) 955.
- [30] T. de Forest, Jr., *Nucl. Phys. A* **392** (1983) 232 .
- [31] Y. Jin, D.S. Onley and L.E. Wright, *Phys. Rev. C* **45** (1992) 1311.
- [32] J.M. Udias, P. Sarriguren, E. Moya de Guerra, E. Garrido and J.A. Caballero, *Phys. Rev. C* **51** (1995) 3246.
- [33] J.M. Udias, P. Sarriguren, E. Moya de Guerra, E. Garrido and J.A. Caballero, *Phys. Rev. C* **48** (1993) 2731.
- [34] S. Frullani and J. Mougey, *Adv. Nucl. Phys.* **14** (1984) 1.
- [35] J. M. Udias, Ph.D. Thesis, Universidad Autonoma (Madrid 1993).
- [36] J.D. Bjorken and S.D. Drell in *Relativistic Quantum Mechanics*, (McGraw Hill, New York, 1964).
- [37] S. Boffi, C. Giusti and F.D. Pacati, *Phys. Rep.* **226** (1993) 1.
- [38] S. Hama, B.C. Clark, E.D. Cooper, H.S. Sherif, and R.L. Mercer, *Phys. Rev.* **C 41** (1990) 2737.
- [39] J.M. Udias, P. Sarriguren, E. Moya de Guerra, and J.A. Caballero, *Phys. Rec. C* **53** (1996) R1488.
- [40] C. R. Chin and A. Picklesimer, *Nuovo Cimento A* **105** (1992) 1149.
- [41] Y. Jin, D.S. Onley, L.E. Wright, *Phys. Rev. C* **50** (1994) 168.
- [42] R. Fritz and H. Müther, *Phys. Rev.* **C 49** (1994) 633.
- [43] A. Bianconi, S. Jeschonnek, N.N. Nikolaev, J. Speth, and B.G. Zakharov, *Phys. Lett.* **B 363** (1995) 217.